

## INTERACTION OF $\text{Fe}(\text{CO})_4$ WITH $\text{C}_{20}$ CAGE IN GAS AND SOLUTION PHASES: A THEORETICAL STUDY

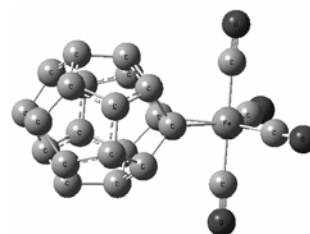
Hanieh ALAVI,<sup>a</sup> Reza GHIASI,<sup>b,\*</sup> Dadkhoda GHAZANFARI<sup>a</sup> and Mohammed Reza AKHGAR<sup>a</sup>

<sup>a</sup>Department of Chemistry, Kerman Branch, Kerman, Islamic Azad University, Kerman, Iran

<sup>b</sup>Department of Chemistry, East Tehran Branch, Islamic Azad University, Qiam Dasht, Tehran, Iran

Received September 19, 2014

In this work, the interaction of  $\text{C}_{20}$  and  $\text{Fe}(\text{CO})_4$  fragment was investigated by MPW1PW91 method in both gas and solution phases. The influence of solvent on the interaction energy, structural parameters, frontier orbital energies and hyperpolarizability of  $\text{C}_{20}\dots\text{Fe}(\text{CO})_4$  complex has been explored. The thermodynamic properties of the  $\text{C}_{20}\dots\text{Fe}(\text{CO})_4$  compound at different temperatures have been calculated. The density of states (DOS) was beneficially used to analyze the main features of electronic structure.



### INTRODUCTION

$\text{C}_{20}$  molecule is potentially the smallest fullerene, and its structure has been investigated theoretically and experimentally.<sup>1-6</sup> This molecule has been generated and characterized in the gas phase.<sup>7</sup> Owing to its attractive structure, this ambiguous molecule has been the subject of many theoretical investigations.<sup>8-9</sup> Fullerenes are considered as promising candidates for basic elements in nanoscale devices, and several examples of fullerene-based devices have been already investigated both experimentally and theoretically.<sup>10-11</sup> Modification of  $\text{C}_{20}$  is a matter of general interest for experimentalists as well theoreticians to look into the structural as well as electronic properties. As a recent research, for instance, structure and properties of fullerene  $\text{C}_{20}$  and its derivatives  $\text{C}_{20}(\text{C}_2\text{H}_2)_n$  and  $\text{C}_{20}(\text{C}_2\text{H}_4)_n$  ( $n=1-4$ ) have been studied.<sup>12</sup> These calculations showed that the most stable fullerene  $\text{C}_{20}$  and its derivatives  $\text{C}_{20}(\text{C}_2\text{H}_2)_n$  and  $\text{C}_{20}(\text{C}_2\text{H}_4)_n$  ( $n=1-3$ ) reveal significant aromaticity, while  $\text{C}_{20}(\text{C}_2\text{H}_2)_4$

and  $\text{C}_{20}(\text{C}_2\text{H}_4)_4$  have no spherical aromaticity. Also, heteroatom impacts on structure, stability and aromaticity of  $\text{X}_n\text{C}_{20-n}$  fullerenes have been explored.<sup>13</sup> The interaction of  $\text{C}_{20}$  with  $\text{N}_2\text{X}_2$  ( $\text{X}=\text{H}, \text{F}, \text{Cl}, \text{Br}, \text{Me}$ ) have been investigated theoretically.<sup>14</sup> Structure, aromaticity, frontier orbital analysis and the natural bond analysis of  $\text{C}_{20}\dots\text{N}_2\text{X}_2$  complexes have been explored, and the influence of the basis set and methods on the structure and interaction energies of these complexes have been explored.

$[\text{Fe}(\text{CO})_4]$  is a coordinatively unsaturated intermediate which generally produced from the stable compound  $[\text{Fe}(\text{CO})_5]$ . The structure and reactions of  $[\text{Fe}(\text{CO})_4]$  were first recognized by IR spectroscopy and matrix isolation experiments.<sup>15-18</sup> Many papers have been published in relation to structure, reactivity and properties of it,<sup>19-23</sup> and these papers provide a significant advance in understanding of  $[\text{Fe}(\text{CO})_4]$ . Interaction of  $[\text{Fe}(\text{CO})_4]$  fragment with alkenes has been studied theoretically.<sup>24</sup>

\* Corresponding author: rezaghiasi1353@yahoo.com, rgiasi@iauet.ac.ir

In the present work, interaction of fullerene C<sub>20</sub> and Fe(CO)<sub>4</sub> has been investigated theoretically. Structure, frontier orbital analysis, thermodynamic parameters, and hyperpolarizability have been studied. The influence of the solvent on the structure and studied properties has been explored.

## COMPUTATIONAL METHODS

All calculations were carried out with the Gaussian 03 suite of program.<sup>25</sup> The calculations of systems contain C, and O described by the standard 6-311G(d,p) basis set.<sup>26-29</sup> For iron element standard LANL2DZ basis set<sup>30-32</sup> are used and iron described by effective core potential (ECP) of Wadt and Hay pseudopotential<sup>30</sup> with a doublet- $\xi$  valance using the LANL2DZ. Geometry optimization was performed utilizing with Modified Perdew-Wang Exchange and Correlation (mpw1pw91).<sup>33</sup> The results of calculations for transition metal complexes show that MPW1PW91 functional gives better results than B3LYP.<sup>34-37</sup> A vibrational analysis was performed at each stationary point found, which confirms its identity as an energy minimum.

$$\beta_{tot} = \left[ \left( \beta_{xxx} + \beta_{xyy} + \beta_{xzz} \right)^2 + \left( \beta_{yyy} + \beta_{yzz} + \beta_{yxx} \right)^2 + \left( \beta_{zzz} + \beta_{zxx} + \beta_{zyy} \right)^2 \right]^{0.5}$$

We have studied the solvation effects by using self-consistent reaction field (SCRF) approach, in particular using the polarizable continuum model (PCM).<sup>39</sup> Using this method, the geometry of the studied complex was re-optimized and the hyperpolarizability was calculated by the same functionals and basis sets.

GaussSum 2.2.6.1 was used to prepare total density of state (TDOS) or density of state.<sup>40</sup>

## RESULTS AND DISCUSSION

### 1. Energetic aspects

Fig. 1 shows the molecular structure and atomic numbering of C<sub>20</sub>...Fe(CO)<sub>4</sub> complex. The energies of C<sub>20</sub>...Fe(CO)<sub>4</sub> complex in gas phase and different media by using the PCM model are listed in Table 1. E<sub>T</sub> is the total energy and  $\Delta E_{solv}$  is the stabilization energy by solvents, the relative energy of the title compound in a solvent to that in the gas phase. From Table 1, we can see that the calculated energy is dependent on the size of the

The interaction energy, IE, can be evaluated from the difference between energy of the complex and sum of the energies of the C<sub>20</sub> and Fe(CO)<sub>4</sub>:

$$I.E = E(\text{complex}) - [E(C_{20}) + E(\text{Fe}(\text{CO})_4)]$$

Geometries were optimized at this level of theory without any symmetry constraints followed by the calculations of the first order hyperpolarizabilities. The total static first hyperpolarizability  $\beta$  was obtained from the following relation:

$$\beta_{tot} = \left( \beta_x^2 + \beta_y^2 + \beta_z^2 \right)^{0.5}$$

upon calculating the individual static components

$$\beta_i = \beta_{iii} + \left( \frac{1}{3} \right) \sum_{i \neq j} \left( \beta_{ijj} + \beta_{jji} + \beta_{jii} \right)$$

Due to the Kleinman symmetry:<sup>38</sup>

$$\beta_{xyy} = \beta_{yxy} = \beta_{yyx} ; \beta_{yyz} = \beta_{zyy} = \beta_{zyz}, \dots$$

one finally obtains the equation that has been employed:

dielectric constant of solvents. In the PCM model, the energies E<sub>T</sub> decrease with the increasing dielectric constants of solvents. On the other hand,  $\Delta E_{solv}$  values indicate the increasing of stability in more polar solvents. This is because a dipole in the molecule will induce a dipole in the medium, and the electric field applied to the solute by the solvent (reaction) dipole will in turn interact with the molecular dipole to lead to net stabilization. This suggests that the C<sub>20</sub>...Fe(CO)<sub>4</sub> complex has more stability in polar solvent rather than in the gas phase.

The computed interaction energies (I.E) for C<sub>20</sub>...Fe(CO)<sub>4</sub> complex on gas phase and various solvents have been gathered in Table 1. As seen from Table 1, it is found that interaction energies values decrease from vacuum to different solvents. Fig. 1 presents a good Linear correlation between dielectric constant of solvent and interaction energy of C<sub>20</sub>...Fe(CO)<sub>4</sub> complex. On the other hand, these values are larger in less polarity, as is in agreement with the analyses from the distance of r(M...C).

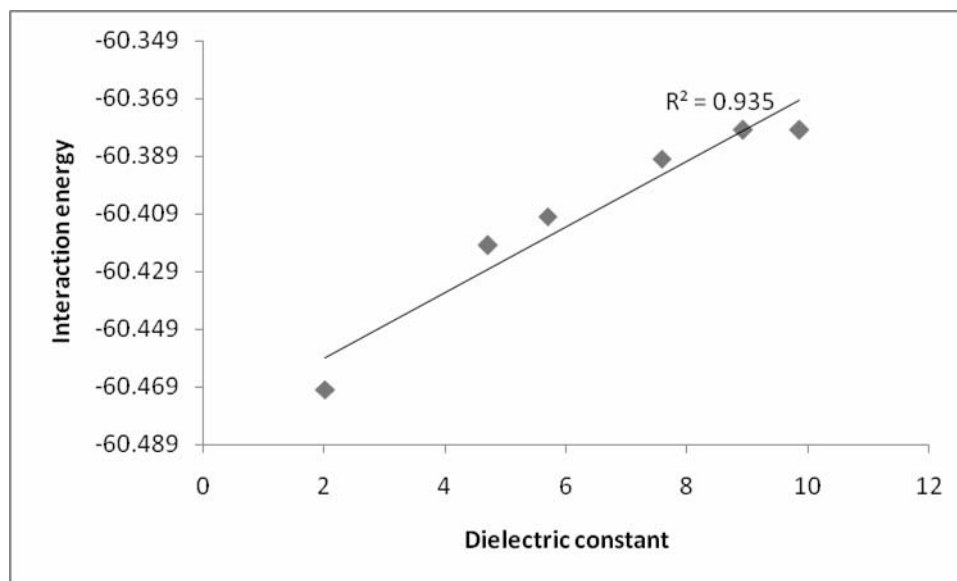


Fig. 1 – Linear correlation between dielectric constant of solvent and interaction energy of C<sub>20</sub>...Fe(CO)<sub>4</sub> complex.

Table 1

Absolute energies (Hartree), dielectric constant of solvents, solvation energies (kcal/mol), interaction energies (kcal/mol), dipole moment (Debye), selected structural parameters (Å) values of C<sub>20</sub>...Fe(CO)<sub>4</sub> complex

phase	$\epsilon$	E(Hartree)	$\Delta E_{\text{solv}}$	IE	$\mu$	M...C	Fe-C <sub>ax</sub>	Fe-C <sub>eq</sub>
gas	-	-1338.3177	-	-60.51	3.9202	2.0201	1.8142	1.7977
CycloHexane	2.0165	-1338.3197	-1.25	-60.47	4.8944	2.0166	1.8152	1.7990
Chloroform	4.7113	-1338.3216	-2.49	-60.42	5.9204	2.0133	1.8162	1.8004
ChloroBenzene	5.6968	-1338.3220	-2.71	-60.41	6.1020	2.0128	1.8164	1.8006
THF	7.58	-1338.3224	-2.97	-60.39	6.3229	2.0121	1.8166	1.8009
MethyleneChloride	8.93	-1338.3226	-3.12	-60.38	6.4552	2.0117	1.8167	1.8011
n-Octanol	9.8629	-1338.3227	-3.19	-60.38	6.5194	2.0115	1.8168	1.8012

## 2. Dipole moment

Dipole moment values of C<sub>20</sub>...Fe(CO)<sub>4</sub> complex in gas phase and different media by using the PCM model are listed in Table 1. These values show the solvent effect on the stabilization energy is in parallel with that on the dipole moment of the solute. Explicitly, there is the larger the dipole moment of solute, and the higher the stabilization energy in the stronger the solvent polarity.

## 3. Bond distances

It is well-known that the solvent polarity influences both the structure and properties of conjugated organic molecules and metal complexes.<sup>41-43</sup> The structural data for the optimized structures of C<sub>20</sub>...Fe(CO)<sub>4</sub> complex in the six studied solvents are collected in Table 1. The results show that the structural parameters are

changed by the polarity of the surrounding media. These values indicate lengthening of Fe-C bonds in the set of solvents rather than gas phase. Also, these values show that Fe-C<sub>ax</sub> and Fe-C<sub>eq</sub> increase with the increasing of dielectric constant of solvent. On the other hand, Fe...C(C<sub>20</sub>) distances are decreasing with the increasing of dielectric constant of solvent.

## 4. Vibrational analysis

The values of most intensities vibrational frequencies of C<sub>20</sub>...Fe(CO)<sub>4</sub> complex are 2151.98, 2174.01, 2221.46, and 2172.32 cm<sup>-1</sup> in gas phase. The vibrational modes of these frequencies are shown in Fig. 2. As can be seen from Fig. 2, these frequencies are attributed to carbonyl stretching frequency.

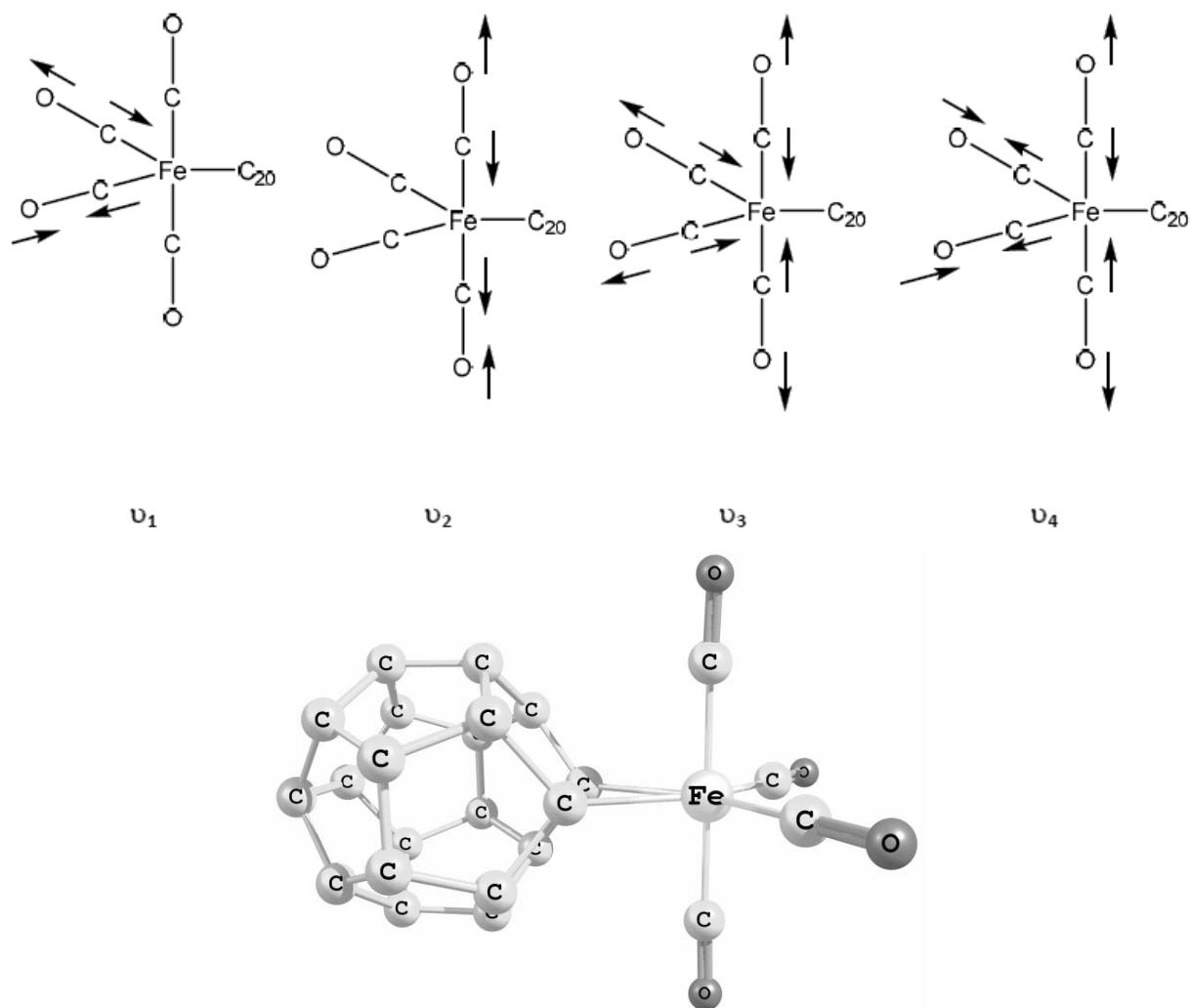


Fig. 2 – The most intensities vibrational frequencies of  $C_{20}\dots Fe(CO)_4$  complex.

Table 2

Frontier orbital energies (in a.u), frontier orbitals gap (in eV), hardness(in eV), softness(in  $eV^{-1}$ ), chemical potential (in eV) and electrophilicity (in eV) values of  $C_{20}\dots Fe(CO)_4$  complex

X	HOMO	LUMO	$\Delta E$	$\eta$	S	$\mu$	$\omega$
gas	-0.20264	-0.10964	2.531	1.265	0.790	-4.249	7.133
CycloHexane	-0.20168	-0.10814	2.545	1.273	0.786	-4.215	6.981
Chloroform	-0.20139	-0.10730	2.560	1.280	0.781	-4.200	6.890
ChloroBenzene	-0.20138	-0.10720	2.563	1.281	0.780	-4.198	6.878
THF	-0.20139	-0.10709	2.566	1.283	0.779	-4.197	6.865
MethyleneChloride	-0.20139	-0.10703	2.568	1.284	0.779	-4.196	6.858
n-Octanol	-0.20140	-0.10700	2.569	1.284	0.779	-4.196	6.854

## 5. Molecular orbital analysis

The energies of the frontier orbitals (HOMO, LUMO) along with the corresponding HOMO–LUMO energy gaps, Hardness, chemical potential, and electrophilicity of  $C_{20}\dots Fe(CO)_4$  complex are given in Table 2. Frontier orbital analysis presents

the HOMO and LUMO are distributed on cage (Fig. 3 (a)). The calculated HOMO and LUMO energies of  $C_{20}\dots Fe(CO)_4$  are at -0.20264 and -0.10964 Hartree, respectively. This yields an HOMO–LUMO energy gap of 2.53 eV.

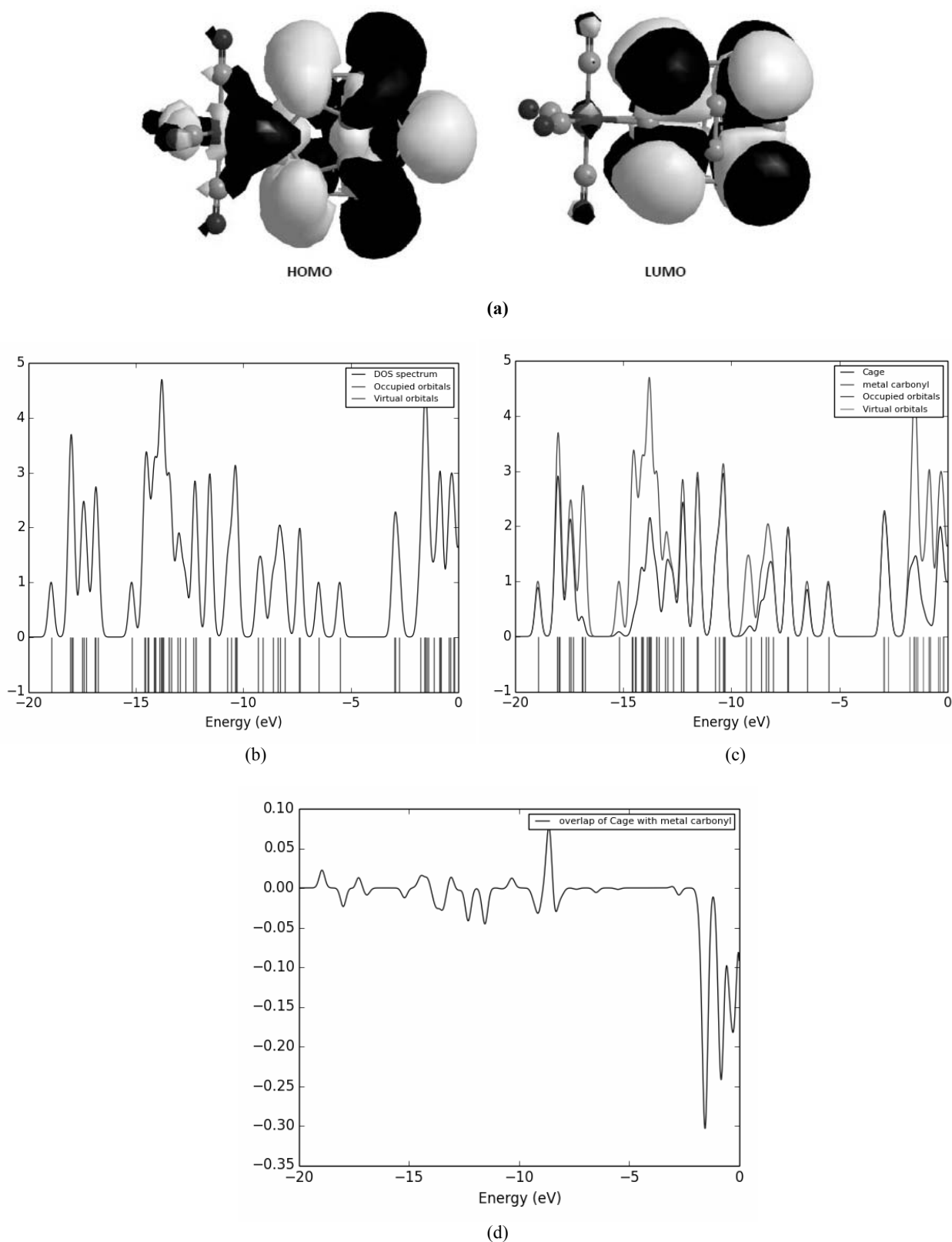


Fig. 3 – (a) Frontier orbitals diagrams, (b) The calculated total electronic density of states (DOS) diagrams, (c) the calculated partial electronic density of states diagrams (PDOS), and (d) crystal orbital overlap population (COOP) for  $\text{C}_{20}\dots\text{Fe}(\text{CO})_4$  complex.

Inclusion of solvation effects also leads to changes on the molecular orbital energies

(Table 2). In solution phase with respect to the corresponding values in vacuum, HOMO and

LUMO are destabilized. Moreover, hardness and chemical potential values have an increase in solution phase. On the other hand, electrophilicity values have been decreased in solution phase.

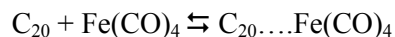
To understand the central features of bonding interactions of compounds, we performed total density of states (TDOS), partial density of states (PDOS), and crystal orbital overlap population (COOP). The DOS, PDOS, and COOP of  $C_{20}\dots Fe(CO)_4$  is sketched in Fig. 3(b).

The PDOS essentially indicates the composition of the fragment orbitals contributing to the molecular orbitals. As clearly shown in this figure, the PDOS reveals that the HOMO and LUMO are fairly localized on cage with fewer contributions from  $Fe(CO)_4$  fragment.

The OPDOS illustrates the nonbonding, bonding and antibonding natures of the interaction between the two atoms, orbitals or groups. Zero value of the OPDOS indicates nonbonding interactions. The positive and negative values indicate the bonding and anti-bonding interaction. In addition, the OPDOS diagrams permit us to resolve and comparison of the donor-acceptor features of the ligand and determine the bonding, and non-bonding.

## 6. Thermodynamic parameters

Thermochemical analysis is studied for  $C_{20}\dots Fe(CO)_4$  complex. The calculated values of  $\Delta G$ ,  $\Delta H$ ,  $\Delta S$ , and  $K$ , in which the individual terms are referred to a temperature of 298 K are -177.99 kJ/mol, -0.21 kcal/mol.K, -241.10 kcal/mol,  $1.58 \times 10^{31}$ , respectively. The reaction can be considered as:



As can be verified, the  $\Delta S$  values are similar for all complexes. Since in this reaction two particles form one,  $\Delta S$  should be a negative value. However, the relative difference of the  $\Delta G$  is almost as same as the  $\Delta H$ .

According to the statistical thermodynamic principle, heat capacities ( $C_v$ , m in  $\text{cal K}^{-1} \text{mol}^{-1}$ ), entropies ( $S$ , in  $\text{cal K}^{-1} \text{mol}^{-1}$ ), and enthalpies ( $H$ , in  $\text{kcal mol}^{-1}$ ) in ranging from 100 to 10000 K were obtained and are gathered in Table 3. As it is obvious from Table 3, the  $C_v$ ,  $S$ , and  $H$  thermodynamic functions of  $C_{20}\dots Fe(CO)_4$  increase with the increase of temperature. The reason for this is that the vibrational movement is invigorated at the higher temperature and makes more contributions to the thermodynamic functions, although the main contributions are due to the translation and rotation of the molecules at the lower temperature. The relationships between the thermodynamic functions and the temperature in 100–1000 K are expressed as:

$$G = -2E-07 T^2 - 0.0001T - 1338.2; R^2 = 0.9999$$

$$H = 1E-07 T^2 + 6E-05T - 1338.2; R^2 = 0.9991$$

$$S = -7E-05x^2 + 0.290x + 57.80; R^2 = 1$$

$$C_v = -0.0001T^2 + 0.293T - 2.2896; R^2 = 0.9988$$

These equations have been shown in Fig. 4.

Table 3

Standard thermodynamic functions of the  $C_{20}\dots Fe(CO)_4$

T	G (Hartree)	H (Hartree)	S (Cal/Mol.K)	$C_v$ (Cal/Mol.K)
100	-1338.175280	-1338.161440	86.843	25.530
200	-1338.191188	-1338.155323	112.531	48.634
300	-1338.211137	-1338.145266	137.783	73.052
400	-1338.235060	-1338.131640	162.242	93.189
500	-1338.262768	-1338.115177	185.230	108.734
600	-1338.294005	-1338.096553	206.504	120.468
700	-1338.328495	-1338.076301	226.077	129.316
800	-1338.365976	-1338.054816	244.070	136.046
900	-1338.406209	-1338.032389	260.640	141.229
1000	-1338.448980	-1338.009231	275.947	145.276

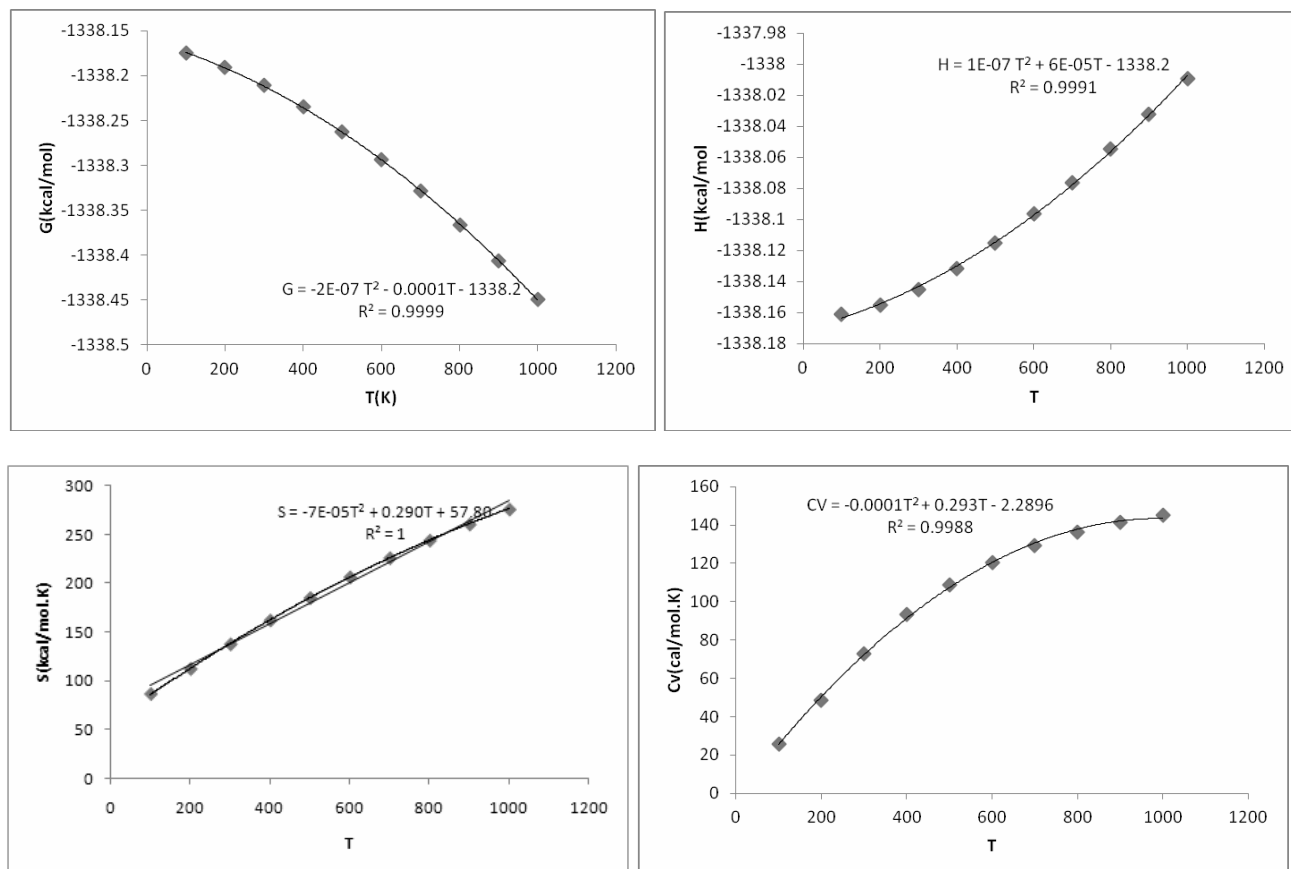


Fig. 4 – The quadratic relationships between the thermodynamic functions and the temperature C<sub>20</sub>...Fe(CO)<sub>4</sub>.

## 7. Hyperpolarizability

Theoretical investigation assists a fundamental role in comprehending of the structure-property correlations, which is able to maintain designing of novel NLO chromophores. The electrostatic first hyperpolarizability ( $\beta_{\text{tot}}$ ) and dipole moment ( $\mu$ ) of the C<sub>20</sub>...Fe(CO)<sub>4</sub> complex have been calculated in both gas phase and various solvents. As can be

seen from Table 4, it is obvious that largest  $\beta_{\text{tot}}$  values are found in higher polarity. Also,  $\beta_{\text{tot}}$  values increase from vacuum phase to different solvents. The dependence of the first hyperpolarizability of the title compound both on the dielectric constant of the media and the Onsager function<sup>44</sup> (Fig. 5) is characteristic for a dipolar reaction field interaction in the solvation process.<sup>45-47</sup>

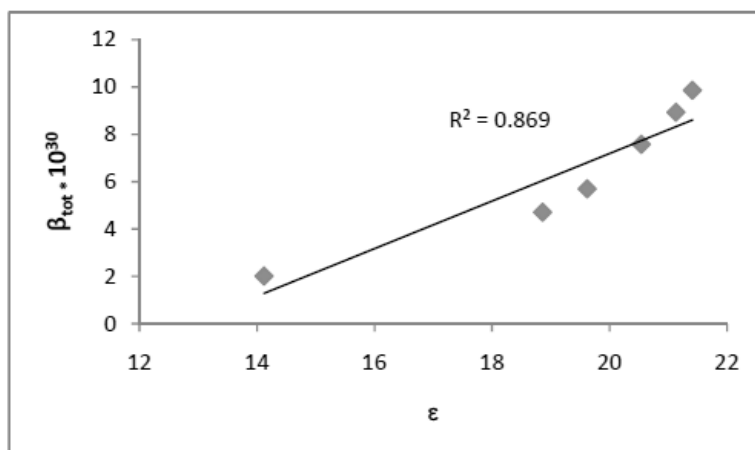
Table 4

$\beta$  components and  $\beta_{\text{tot}}$  values ( $10^{-30}$  esu) for C<sub>20</sub>...Fe(CO)<sub>4</sub> complex in gas phase and various solvents

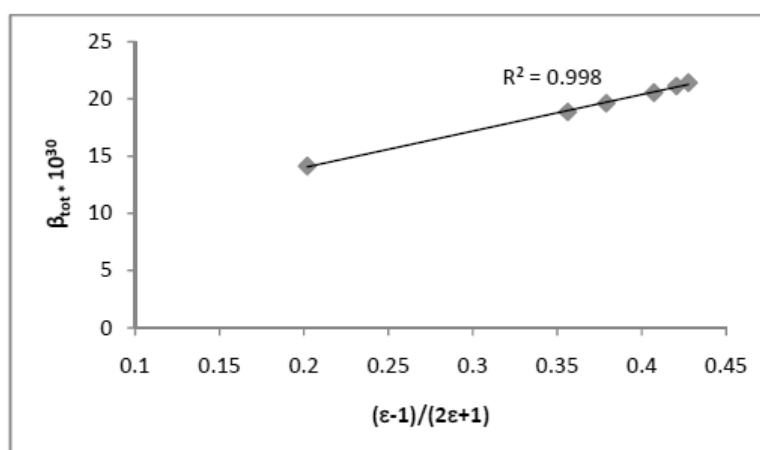
	gas	Cyclohexane	Chloroform	ChloroBenzene	THF	MethyleneChloride	n-Octanol
$\beta_{\text{XXX}}$	-827.65	-1207.16	-1545.12	-1596.90	-1658.02	-1692.69	-1709.18
$\beta_{\text{XXY}}$	-7.42	1.28	-1.11	-1.69	-1.71	-1.58	-1.60
$\beta_{\text{XYY}}$	-63.44	-114.45	-173.42	-186.77	-205.26	-217.28	-223.35
$\beta_{\text{YYV}}$	-23.87	2.57	3.38	3.42	4.07	4.64	4.61
$\beta_{\text{XXZ}}$	-5.45	-7.65	12.14	8.13	0.47	-0.83	-2.00
$\beta_{\text{XVZ}}$	0.56	8.26	-9.44	-9.10	-8.18	-6.90	-6.61
$\beta_{\text{YYZ}}$	8.71	1.12	19.01	15.74	7.58	9.59	6.64
$\beta_{\text{XZZ}}$	-218.36	-312.99	-462.58	-485.94	-513.97	-535.60	-545.88

Table 4 (continued)

$\beta_{YZZ}$	-10.63	0.55	-18.61	-17.30	-7.31	-8.80	-5.68
$\beta_{ZZZ}$	11.18	-6.55	45.35	40.20	13.86	18.93	10.23
$\beta_{tot}$	9.59E-30	1.41E-29	1.89E-29	1.96E-29	2.05E-29	2.11E-29	2.14E-29
$\beta_{tot} \times 10^{30}$	9.59	14.12	18.86	19.62	20.54	21.13	21.41



(a)



(b)

Fig. 5 – Dependence of  $\beta_{tot}$  for  $C_{20}...Fe(CO)_4$  compound on the dielectric constant (a) and Onsager function (b).

## CONCLUSIONS

We showed in paper:

The interaction energies values decrease from vacuum to different solvents.

The strongest stretching frequencies of complex are attributed to carbonyl stretching frequencies.

In solution, HOMO and LUMO energies, hardness and chemical potential values are increased, with respect to the corresponding values in vacuum. On the other hand, electrophilicity values have been decreased in solution phase.

The largest  $\beta_{tot}$  values have been found in more polarity, and these values increase from vacuum to different solvents.

## REFERENCES

1. J. C. Grossman, L. Mitas and K. Raghavachari, *Phys. Rev. Lett.*, **1995**, 750, 3870.
2. E. J. Bylaska, P. R. Taylor, R. Kawai and J. H. Weare, *J. Phys. Chem. A*, **1996**, 100, 6966.
3. R. Taylor, E. Bylaska, J. H. Weare and R. Kawai, *Chem. Phys. Lett.*, **1995**, 235, 558.



4. Z. Wang, P. Day and R. Pachte, *Chem. Phys. Lett.*, **1996**, 248, 121.
5. M. L. M. Jan, J. El-Yazal and J. Francois, *Chem. Phys. Lett.*, **1996**, 248, 345.
6. S. Sokolova, A. Luchow and J. B. Anderson, *Chem. Phys. Lett.*, **2000**, 323, 229.
7. H. Prinzbach, A. Weiler, P. Landenberger, F. Wahl, J. Worth, L. T. Scott, M. D. Gelmont, D. Olevano and B. V. Issendorff, *Nature*, **2000**, 60, 407.
8. J. Luo, L. M. Peng, Z. Q. Xue and J. L. Wu, *J. Chem. Phys.*, **2004**, 120, 7998.
9. Z. Chen, T. Heine, H. Jiao, A. Hirsch, W. Thiel and P. V. R. Schleyer, *Chem. Eur. J.*, **2004**, 10, 963.
10. J. Taylor, H. Guo and J. Wang, *Phys. Rev. B*, **2001**, 63, 121104.
11. D. Zeng, H. Wang, B. Wang and J. G. Hou, *Appl. Phys. Lett.*, **2000**, 77, 3595.
12. C. Zhang, W. Sun and Z. Caob, *J. Chem. Physics*, **2007**, 126, 144306.
13. M. Z. Kassae, F. Buazar and M. Koochi, *J. Molec. Struct.: THEOCHEM*, **2010**, 940, 19.
14. R. Ghiasi, M. Z. Fashami and A. H. N. Hakimion, *J. Theoretic. Computational Chem.*, **2014**, 13, 1450023.
15. M. Poliakoff and J. J. Turner, *J. Chem. Soc. Dalton Trans.*, **1973**, 1351.
16. M. Poliakoff and J. J. Turner, *J. Chem. Soc. Dalton Trans.*, **1974**, 2276.
17. T. J. Barton, R. Grinter, A. J. Thomson, B. Davies and M. Poliakoff, *J. Chem. Soc. Chem. Commun.*, **1977**, 841.
18. M. Poliakoff and E. Weitz, *Acc. Chem. Res.*, **1987**, 20, 408.
19. M. Poliakoff and J. J. Turner, *Angew. Chem. Int. Ed.*, **2001**, 40, 2809.
20. H. Ihee, J. Cao and A. H. Zewail, *Angew. Chem. Int. Ed.*, **2001**, 40, 1532.
21. S. A. Trushin, W. Fuss, K. L. Kompa and W. E. Schmid, *J. Phys. Chem. A*, **2000**, 104, 1997.
22. P. T. Snee, C. K. Payne, K. T. Kotz, H. Yang and C. B. Harris, *J. Am. Chem. Soc.*, **2001**, 123, 2255.
23. N. Leadbeater, *Coord. Chem. Rev.*, **1999**, 188, 35.
24. R. Hoffmann, T. A. Albright and D. L. Thorn, *Pure & Appl. Chem.*, **50**, 1.
25. M. J. Frisch, G. W. Trucks, H. B. Schlegel, G. E. Scuseria, M. A. Robb, J. R. Cheeseman, J. A. Montgomery, Jr., T. Vreven, K. N. Kudin, J. C. Burant, J. M. Millam, S. S. Iyengar, J. Tomasi, V. Barone, B. Mennucci, M. Cossi, G. Scalmani, N. Rega, G. A. Petersson, H. Nakatsuji, M. Hada, M. Ehara, K. Toyota, R. Fukuda, J. Hasegawa, M. Ishida, T. Nakajima, Y. Honda, O. Kitao, H. Nakai, M. Klene, X. Li, J. E. Knox, H. P. Hratchian, J. B. Cross, C. Adamo, J. Jaramillo, R. Gomperts, R. E. Stratmann, O. Yazyev, A. J. Austin, R. Cammi, C. Pomelli, J. W. Ochterski, P. Y. Ayala, K. Morokuma, G. A. Voth, P. Salvador, J. J. Dannenberg, V. G. Zakrzewski, S. Dapprich, A. D. Daniels, M. C. Strain, O. Farkas, D. K. Malick, A. D. Rabuck, K. Raghavachari, J. B. Foresman, J. V. Ortiz, Q. Cui, A. G. Baboul, S. Clifford, J. Cioslowski, B. B. Stefanov, G. Liu, A. Liashenko, P. Piskorz, I. Komaromi, R. L. Martin, D. J. Fox, T. Keith, M. A. Al-Laham, C. Y. Peng, A. Nanayakkara, M. Challacombe, P. M. W. Gill, B. Johnson, W. Chen, M. W. Wong, C. Gonzalez and J. A. Pople, Revision B.03 ed., Gaussian, Inc., Pittsburgh PA., **2003**.
26. R. Krishnan, J. S. Binkley, R. Seeger and J. A. Pople, *J. Chem. Phys.*, **1980**, 72, 650.
27. A. J. H. Wachters, *J. Chem. Phys.*, **1970**, 52, 1033.
28. P. J. Hay, *J. Chem. Phys.*, **1977**, 66, 4377.
29. A. D. McLean and G. S. Chandler, *J. Chem. Phys.*, **1980**, 72, 5639.
30. P. J. Hay and W. R. Wadt, *J. Chem. Phys.*, **1985**, 82, 299.
31. P. J. Hay, W. R. Wadt, *J. Chem. Phys.*, **1985**, 82, 284.
32. A. Schaefer, H. Horn and R. Ahlrichs, *J. Chem. Phys.*, **1992**, 97, 2571.
33. C. Adamo, V. Barone, *J. Chem. Phys.*, **1998**, 108, 664.
34. J. P. C. A. M. Porembski and J. C. Weisshaar, *J. Phys. Chem. A*, **2001**, 105, 4851.
35. M. Porembski and J. C. Weisshaar, *J. Phys. Chem. A*, **2001**, 105, 6655.
36. Y. Zhang, Z. Guo and X.-Z. You, *J. Am. Chem. Soc.*, **2001**, 123, 9378.
37. R. C. Dunbar, *J. Phys. Chem. A* **2002**, 106, 7328.
38. D. A. Keleman, *Phys. Rev.*, **1962**, 126, 1977.
39. J. Tomasi, B. Mennucci and R. Cammi, *Chem. Rev.*, **2005**, 105, 2999.
40. N. M. O'Boyle, A. L. Tenderholt and K. M. Langner, *J. Comp. Chem.*, **2008**, 29, 839.
41. P. J. Mendes, T. J. L. Silva, A. J. P. Carvalho and J. P. P. Ramalho, *J. Molec. Structure: THEOCHEM*, **2010**, 946, 33.
42. L. M. Chen, J. C. Chen, H. Luo, S. Y. Liao and K. C. Zheng, *J. Theoretical and Computational Chem.*, **2011**, 10, 581.
43. X. Cao, C. Liu and Y. Liu, *J. Theoretical and Computational Chem.*, **2012**, 11, 573.
44. L. Onsager, *J. Am. Chem. Soc.*, **1936**, 58, 1486.
45. P. C. Ray and J. Leszczynski, *Chem. Phys. Lett.*, **2004**, 339.
46. K. Clays and A. Persoons, *Phys. Rev. Lett.*, **1991**, 66, 2980.
47. H. Lee, S.-Y. An and M. Cho, *J. Phys. Chem. B*, **1999**, 103, 4992.

